Numerical Study of Bidimensional Steady Natural Convection in a Space Annulus Between Two Elliptic Confocal Ducts Influence of the Internal Eccentricity

Mahfoud Djezzar [1], Abla Chaker [1] and Michel Daguenet [2]

[1] Laboratoire de Physique Energétique, Département de Physique, Faculté des Sciences, Université Mentouri Constantine, Algérie

[2] Université de Perpignan, 52 Avenue de Villeneuve, 66860 Perpignan cedex, France

Résumé - *Les auteurs expriment les équations de Boussinesq de la convection naturelle thermique laminaire permanente et bidimensionnelle. Ils proposent un nouveau code de calcul aux volumes finis qui utilise les fonctions primitives (formulation vitesse-pression) et un système de coordonnées elliptiques. Le nombre de Prandtl est fixé à 0.7 (cas de l'air) mais le nombre de Rayleigh varie. Ils examinent l'effet de la géométrie du cylindre elliptique intérieur sur les résultats obtenus.*

Abstract - *The authors express the Boussinesq equations of the laminar thermal and natural convection, in the case of permanent and bidimensional flow, in an annular space between two confocal elliptic cylinders. A new calculation code using the finite volumes with the primitive functions (velocity-pressure formulation) and the elliptic coordinates system is proposed. The Prandtl number is fixed at 0.7 (case of the air) with varying the Rayleigh number. The effect of the geometry of the interior elliptic cylinder on the results is examined.*

Keywords: Natural convection - Boussinesq equations - Annular space - Elliptic cylinders - Velocity - Pressure formulation.

1. INTRODUCTION

Heat transfer by natural convection, in an annular space delimited by two concentric or eccentric horizontal cylinders, was the subject of many theoretical and experimental studies because of their importance in many engineering applications.

The majority of these studies are related to cylinders, whose cross-sections are circular. Mack and Bishop [1] made a study in an annular space ranging between two horizontal concentric cylinders. They employed a power series truncated at the third power of the Rayleigh number to represent the stream function and temperature variables. The work of Kuehn and Goldstein [2] can be referred as a comprehensive review for concentric cases. They compared the obtained experimental and numerical results using a method with finite differences.

Comparatively, fewer publications were found for natural convection in non-circular domain, e.g., the elliptic domain considered in this study. Lee and Lee [3] attempted to formulate the free convection problem in terms of elliptical coordinates for the symmetrical cases of oblate and prolate elliptical annuli. Elshamy et al [4] studied numerically the case in the horizontal confocal elliptical annulus and developed some practical correlations for the average Nusselt number. Chmaissem et al [5] simulated the case of natural convection in an annular space: having a horizontal axis bounded by circular and elliptical isothermal cylinders. Cheng and Chao [6] employed the body-fitted coordinate transformation method to generate a non-staggered curvilinear coordinate system and performed numerical study for some horizontal eccentric elliptical annuli.

In the numerical simulation of natural convection in elliptical space annuli, finite difference, finite volume and finite element methods were usually used with the vorticity-stream function formulation. For example, the work of Guj and Stella [7] was conducted by the finite difference method, Chmaissem et al [5] used the finite element method, Elshamy et al [4] and Cheng and Chao [6] used the finite volume method, and in the study of Zhu et al [8] the natural convective heat transfer was simulated using the differential quadrature (DQ) method.

In this work we use a new calculation code with the finite volumes [9] which uses the elliptic coordinates and the primitive functions (velocity-pressure formulation), associated to traditional SIMPLER algorithm [9], in order to resolve our system of equations. The grid is made of 130 x 60 nodes.

2. PROBLEM FORMULATION AND BASIC EQUATIONS

Let's consider an annular space, filled with a Newtonian fluid, and located between two confocal elliptic cylinders of horizontal axes. (Fig. 1) represents a cross-section of the system. Both internal and external walls are maintained respectively at the temperatures T_1 and T_2 with $T_1 > T_2$. The physical properties of the fluid are constant, apart from the density ρ whose variations are at the origin of the natural convection. Viscous dissipation is neglected, just as the radiation (emissive properties of the two walls being neglected). We admit that the problem is bidimensional, permanent and laminar.
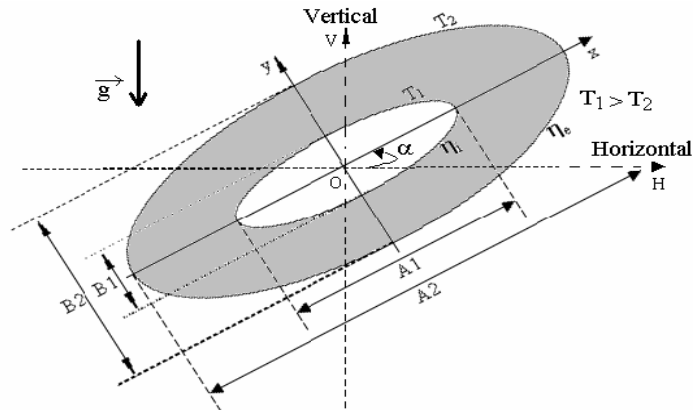

Fig. 1: A cross-section of the system

The laminar natural convection equations within the framework of the Boussinesq approximation are written in vectorial form:

- Continuity equation : $$\mathrm{div}\ \vec{V} = 0 \tag{1}$$

- Momentum equation : $$\vec{V} \cdot \overrightarrow{\mathrm{grad}}\ \vec{V} = \frac{\rho}{\rho_0}\ \vec{g} + \frac{\nabla \pi}{\rho_0} \tag{2}$$

- Heat equation : $$\vec{V} \cdot \overrightarrow{\mathrm{grad}} T = \frac{\lambda}{\rho c_p} \nabla^2 T \tag{3}$$

It is convenient to define a reference frame such as the limits of the system result in constant values of the coordinates. The coordinates known as "elliptic" (η, θ) allow in our case to obtain precisely this result. The wall of the external elliptic cylinder is represented by $\eta = \eta_2 = $ constant, while for the interior elliptic cylinder by $\eta = \eta_1 = $ constant.

The passage of the Cartesian coordinates to the elliptic coordinates is obtained by the following relations :

$$\{ \; x = a\,\mathrm{ch}\,\eta\,\cos\theta \quad \text{and} \quad y = a\,\mathrm{sh}\,\eta\,\sin\theta \; \} \tag{4}$$

The metric coefficients in elliptic coordinates are given by :

$$\{ \; h_1 = h_2 = h = a(\mathrm{sh}^2\,\eta + \sin^2\theta)^{1/2} \quad \text{and} \quad h_3 = 1 \} \tag{5}$$

with :
$$a = \frac{A_1}{\mathrm{ch}\,\eta_1} = \frac{B_1}{\mathrm{sh}\,\eta_1} = \frac{A_2}{\mathrm{ch}\,\eta_2} = \frac{B_2}{\mathrm{sh}\,\eta_2} \tag{6}$$

The gravity vector $\vec{g}$ is written in the new system of coordinates as :

$$\vec{g} = -g\left[\frac{a\,(\mathrm{sh}\,\eta\,\cos\theta\,\sin\alpha + \mathrm{ch}\,\eta\,\sin\theta\,\cos\alpha)}{h}\vec{e}_\eta + \frac{a\,(\mathrm{sh}\,\eta\,\cos\theta\,\cos\alpha - \mathrm{ch}\,\eta\,\sin\theta\,\sin\alpha)}{h}\vec{e}_\theta\right] \tag{7}$$

The dimensionless equations are written by posing the following dimensionless quantities :

$$h^* = \frac{h}{a} = (\mathrm{sh}^2\,\eta + \sin^2\theta)^{1/2} \quad , \quad V_\eta^* = \frac{V_\eta}{\left(\nu/a\right)} \quad , \quad V_\theta^* = \frac{V_\theta}{\left(\nu/a\right)},$$

$$P^* = \frac{P - P_0}{\left(\nu^2/a^2\right)} \qquad \text{and} \qquad T^* = \frac{T - T_2}{T_1 - T_2}$$

a is the characteristic length and **ν/a** is the characteristic velocity.

So let us introduce the following dimensionless numbers :

The Prandtl number, $Pr = \dfrac{\nu\,\rho\,c_p}{\lambda}$ and the Grashof number, $Gr = \dfrac{g\beta a^3}{\nu^2}\Delta T$

After some lengthy manipulations, the following set of equations, is obtained :

Equation (1) becomes :
$$\frac{\partial}{\partial\eta}(h^* V_\eta^*) + \frac{\partial}{\partial\theta}(h^* V_\theta^*) = 0 \tag{8}$$

Projection of equation (2) following the η axis gives :

$$\left[\frac{\partial}{\partial\eta}(h^* V_\eta^* V_\eta^*) + \frac{\partial}{\partial\theta}(h^* V_\eta^* V_\theta^*)\right] = -h^*\frac{\partial P^*}{\partial\eta} + Gr\,T^*\,h^*\left(\mathrm{sh}\,\eta\,\cos\theta\,\sin\alpha + \mathrm{ch}\,\eta\,\sin\theta\,\cos\alpha\right)$$

$$+ 2\frac{\partial^2 V_\eta^*}{\partial\eta^2} + \frac{\partial^2 V_\eta^*}{\partial\theta^2} - \frac{\partial}{\partial\theta}\left[\frac{V_\eta^*}{h^*}\frac{\partial h^*}{\partial\theta}\right] + 2\frac{\partial}{\partial\eta}\left[\frac{V_\theta^*}{h^*}\frac{\partial h^*}{\partial\theta}\right] + \frac{\partial}{\partial\theta}\left[h^*\frac{\partial}{\partial\eta}\left(\frac{V_\theta^*}{h^*}\right)\right] \tag{9}$$

$$+ \left[\frac{\partial}{\partial\eta}\left(\frac{V_\theta^*}{h^*}\right) + \frac{\partial}{\partial\theta}\left(\frac{V_\eta^*}{h^*}\right)\right]\frac{\partial h^*}{\partial\eta} - 2\left[\frac{1}{h^*}\frac{\partial V_\theta^*}{\partial\theta} + \frac{V_\eta^*}{h^{*2}}\frac{\partial h^*}{\partial\eta}\right]\frac{\partial h^*}{\partial\eta} + V_\theta^{*2}\frac{\partial h^*}{\partial\eta} - V_\eta^* V_\theta^*\frac{\partial h^*}{\partial\eta}$$

and following the θ axis, it gives:

$$\left[\frac{\partial}{\partial\eta}(h^* V_\eta^* V_\theta^*) + \frac{\partial}{\partial\theta}(h^* V_\theta^* V_\theta^*)\right] = -h^*\frac{\partial P^*}{\partial\theta} + Gr\,T^*\,h^*\left(\mathrm{sh}\,\eta\,\cos\theta\,\cos\alpha - \mathrm{ch}\,\eta\,\sin\theta\,\sin\alpha\right)$$

$$+ 2\frac{\partial^2 V_\theta^*}{\partial\theta^2} + \frac{\partial^2 V_\theta^*}{\partial\eta^2} - \frac{\partial}{\partial\eta}\left[\frac{V_\theta^*}{h^*}\frac{\partial h^*}{\partial\eta}\right] + 2\frac{\partial}{\partial\theta}\left[\frac{V_\eta^*}{h^*}\frac{\partial h^*}{\partial\eta}\right] + \left[\frac{\partial}{\partial\eta}\left(\frac{V_\theta^*}{h^*}\right) + \frac{\partial}{\partial\theta}\left(\frac{V_\eta^*}{h^*}\right)\right]\frac{\partial h^*}{\partial\eta} \tag{10}$$

$$- 2\left[\frac{1}{h^*}\frac{\partial V_\eta^*}{\partial\eta} + \frac{V_\theta^*}{h^{*2}}\frac{\partial h^*}{\partial\theta}\right]\frac{\partial h^*}{\partial\theta} + V_\eta^{*2}\frac{\partial h^*}{\partial\eta} - V_\eta^* V_\theta^*\frac{\partial h^*}{\partial\eta} + \frac{\partial}{\partial\eta}\left[h^*\frac{\partial}{\partial\theta}\left(\frac{V_\eta^*}{h^*}\right)\right]$$

and finally equation (3) becomes :

$$\left[\frac{\partial}{\partial \eta}(h^* V_\eta^* T^*) + \frac{\partial}{\partial \theta}(h^* V_\theta^* T^*)\right] = \frac{1}{Pr}\left[\frac{\partial^2 T^*}{\partial \eta^2} + \frac{\partial^2 T^*}{\partial \theta^2}\right] \qquad (11)$$

The boundary conditions are the following ones :

- Conditions on the inner surface ($\eta=\eta_i=$ constant):

$$\left\{V_\eta^* = V_\theta^* = 0 \qquad \text{and} \qquad T_1^* = 1\right\} \qquad (12)$$

- Conditions on the outer surface ($\eta = \eta_e =$ constant) :

$$\left\{V_\eta^* = V_\theta^* = 0 \qquad \text{and} \qquad T_2^* = 0\right\} \qquad (13)$$

To evaluate the stream's function values, we use the following relations:

$$\left\{V_\eta^* = \frac{1}{h^*}\frac{\partial \psi^*}{\partial \theta} \qquad \text{and} \qquad V_\theta^* = -\frac{1}{h^*}\frac{\partial \psi^*}{\partial \eta}\right\} \qquad (14)$$

3. NUMERICAL METHOD

To solve equations (9) to (11) with associated boundary conditions equations (12) and (13), we consider a numerical solution by the method of finite volumes, presented by S.V.Patankar [9]. The algorithm of SIMPLER [9] is used for the sequential solution of the system of equations of discretization. The iterative numerical solution of the algebraic system of equations is that of sweeping implying the tridiagonal algorithms of Thomas and cyclic.
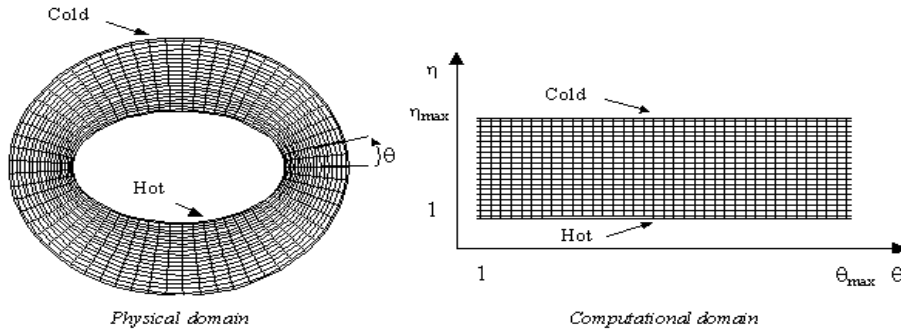

Fig. 2: Physical domain and computational

Figure 2 shows both the physical and the computational domain. Once the temperature distribution is available, the local Nusselt number in the physical domain is defined as :

$$Nu = -\frac{1}{h^*}\frac{\partial T^*}{\partial \eta} \qquad (15)$$

The average Nusselt number is obtained by integrating the local Nusselt numbers around the walls :

$$\overline{Nu} = \frac{1}{2\pi}\int_{-\pi}^{+\pi} Nu \; d\theta \qquad (16)$$

4. RESULTS AND DISCUSSION

We consider three annular spaces characterised by the eccentricity of the internal elliptic tube ($e_1 = 0.999$), ($e_1 = 0.9$) and ($e_1 = 0.83$). The eccentricity of the external elliptic tube is maintained constant ($e_2 = 0.75$). We use four values for the Grashof number Gr (Gr $= 10^3$,

$Gr = 10^4$, $Gr = 10^5$ and $Gr = 2\ 10^5$). The fluid is assumed as air, so the number of Prandtl is supposed to be constant and equal to 0.7.

4.1 Numerical code validation

An annular space ranging between two confocal and horizontal elliptic cylinders [4] has been considered. We present in (Fig. 3), the streamlines and the isotherms resulting from our calculation code with the same parameters used by Elshamy et al [4].
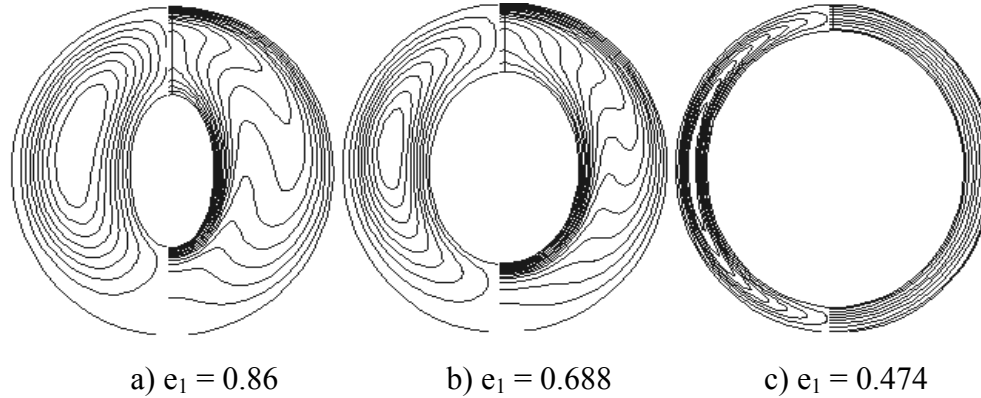

a) $e_1 = 0.86$ b) $e_1 = 0.688$ c) $e_1 = 0.474$

Fig. 3: Streamlines and isotherms for $Ra = 10^4$, $\alpha = 0\ °$ and $e_0 = 0.4$

By comparing this figure with (Fig. 9) and (Fig. 10) of the ref. [4], we can notice, that the results are similar. Further, we gather in the (Table 1), the average Nusselt number's values on the two walls resulting from our calculations and those of the ref. [4].

Furthermore, we can notice that these values are in a good agreement.

Table 1: Comparison of average Nusselt number Ref. [4] with our results

e_1	e_2	Inclinaison	Ra	Internal wall		External wall	
				Ref. [4]	Our results	Ref. [4]	Our results
0.688	0.4	$\alpha = 90\ °$	10^4	2.66	2.72	1.38	1.43
0.388	0.4	$\alpha = 90\ °$	10^4	4.94	4.78	2.51	2.52
0.86	0.4	$\alpha = 90\ °$	10^4	3.68	3.46	1.35	1.30

4.2 The influence of the Grashof number

Figures 4-8 and 9 correspond to $\alpha = 0°$. They represent the isotherms and the streamlines for different Grashof number values. The vertical fictitious plan passing by system centre is a plan of symmetry. The isotherms and the streamlines are symmetrical compared to the vertical plan. On the left side of this plan, the flow turns in the trigonometrical direction. On the right side, the flow is in the opposite direction (the particles of the fluid move upwards, under the action of gravity forces, along the intern hot wall and go down near to the extern cold wall).

When the Grashof number is weak, as being lower or equal to 10^3, the heat transfer is essentially conductive, so the isotherms (Fig .4) have the same form as the walls. Nevertheless there is a movement of the fluid: the particles, which warm up on the wall of the internal elliptic cylinder, tend to rise along this one, then to go down again along the wall of the external elliptic cylinder. Thus the flow is organised in two principal cells which turn very slowly in opposite directions. The laminar convection is weak.
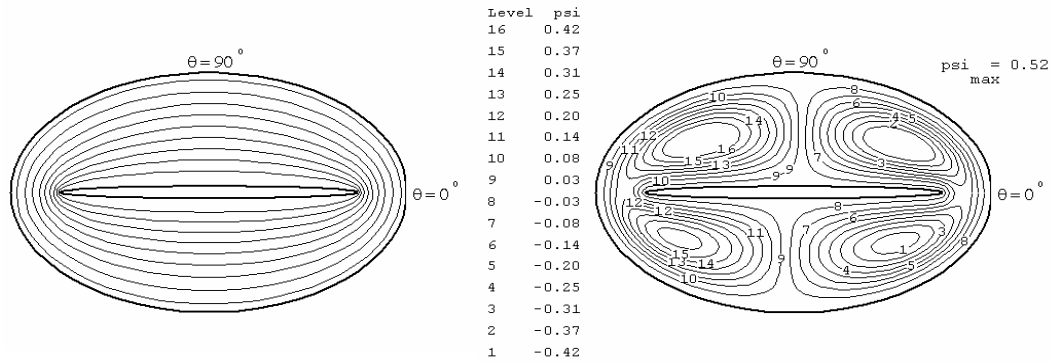
Level	psi
16	0.42
15	0.37
14	0.31
13	0.25
12	0.20
11	0.14
10	0.08
9	0.03
8	-0.03
7	-0.08
6	-0.14
5	-0.20
4	-0.25
3	-0.31
2	-0.37
1	-0.42

Fig. 4: Isotherms and streamlines for Gr = 10^3, α = 0 °, e_1 = 0.999 and e_2 = 0.75

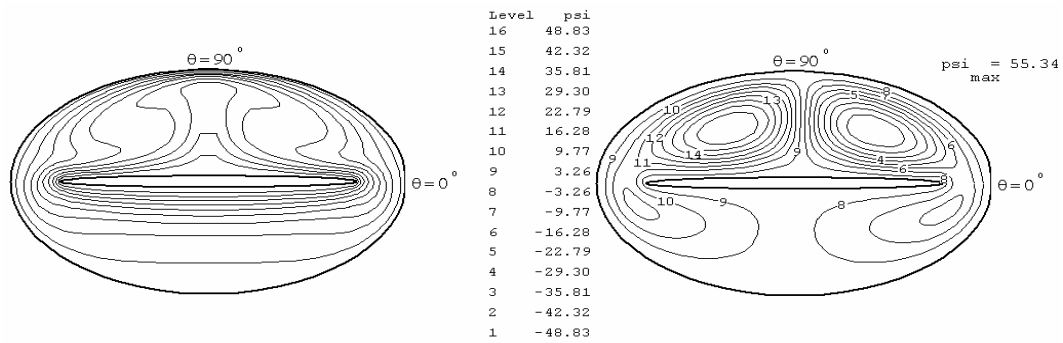| Level	psi
16	48.83
15	42.32
14	35.81
13	29.30
12	22.79
11	16.28
10	9.77
9	3.26
8	-3.26
7	-9.77
6	-16.28
5	-22.79
4	-29.30
3	-35.81
2	-42.32
1	-48.83

Fig. 5: Isotherms and streamlines for Gr = 10^5, α = 0 °, e_1 = 0.999 and e_2 = 0.75

When the Grashof number increases to 10^5 (fig .5) shows that the streamlines values increase, the flow which is going up on the side of the hot wall and going down on the side of the cold wall, becomes intense and the natural convection is dominant. The isotherms become deformed and inserted at the top where the convection is strong.

The variation ΔT^* between the isotherms of (Figs. 4-6) is equal to 0.1 and the values of the streamlines are given on these figures.

For Gr = 2 10^5, the streamlines values show an appreciable increase in the flow. This means that the convection becomes more important and predominates on the conduction. The flow of the fluid becomes multicellular. Both in the left side and in the right side of the annular space, a secondary flow is done in opposite direction of the principal cell, (Fig .6). It seems to us that the geometry of the two walls is at the origin of the formation of secondary flow, by increasing the number of Grashof, the two secondary cells turn between two horizontal planes in the top region of the annular space. The transfer is done primarily by convection.
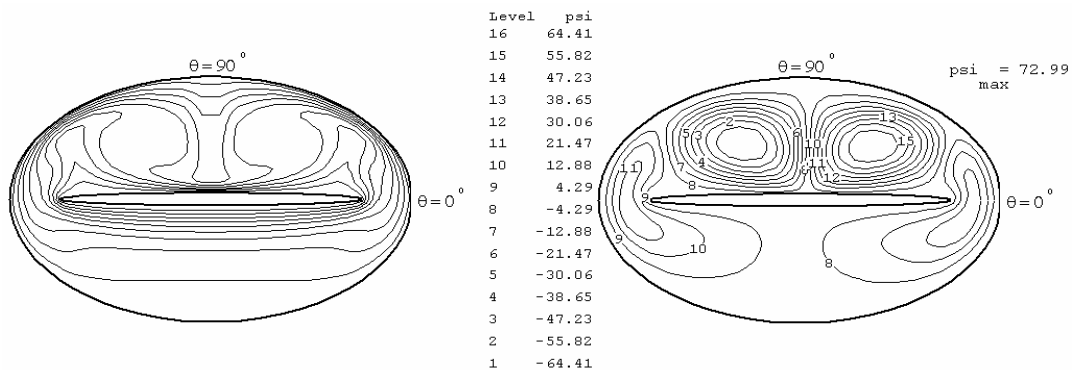
Level	psi
16	64.41
15	55.82
14	47.23
13	38.65
12	30.06
11	21.47
10	12.88
9	4.29
8	-4.29
7	-12.88
6	-21.47
5	-30.06
4	-38.65
3	-47.23
2	-55.82
1	-64.41

Fig. 6: Isotherms and streamlines for Gr = 2 10^5, α = 0 °, e_1 = 0.999 and e_2 = 0.75

4.3 The influence of the internal eccentricity

The variation of the internal eccentricity has a considerable effect both on the fields of flow and temperature. We can already notice that for the same value of the Grashof number $Gr = 10^5$, (Fig. 5) and (Fig. 7) show the influence of the internal eccentricity, the fluid which was bicellular for $e_1 = 0.999$ becomes multicellular for $e_1 = 0.9$.

When $Gr = 2 \cdot 10^5$, the comparison of (Fig. 6) for $e_1 = 0.999$ with (Fig. 8) for $e_1 = 0.9$, shows that the variation of the internal eccentricity modifies the flow and its intensity: Initially there is one bifurcation (Fig. 6) and after, we can notice two bifurcations (Fig.8) in annular space. We also notice that for $e_1 = 0.83$ (Fig. 9) there is no bifurcation.

Variation ΔT^* between the isotherms of (Fig. 7-9) is equal to 0.1 too and the values of the streamlines are given on these figures.
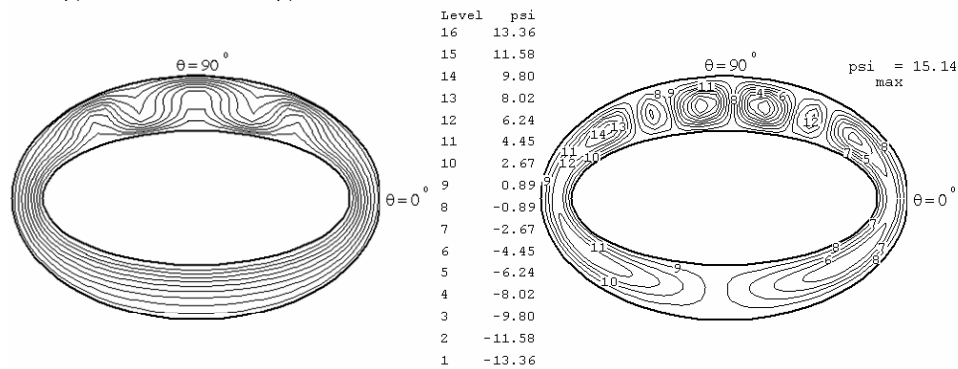

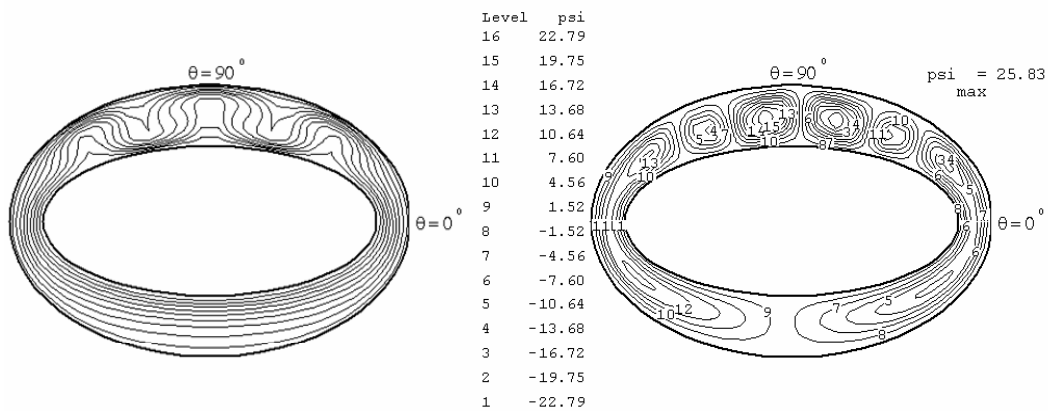Fig. 7: Isotherms and streamlines for $Gr = 10^5$, $\alpha = 0°$, $e_1 = 0.9$ and $e_2 = 0.75$

Fig. 8: Isotherms and streamlines for $Gr = 2 \cdot 10^5$, $\alpha = 0°$, $e_1 = 0.9$ and $e_2 = 0.75$

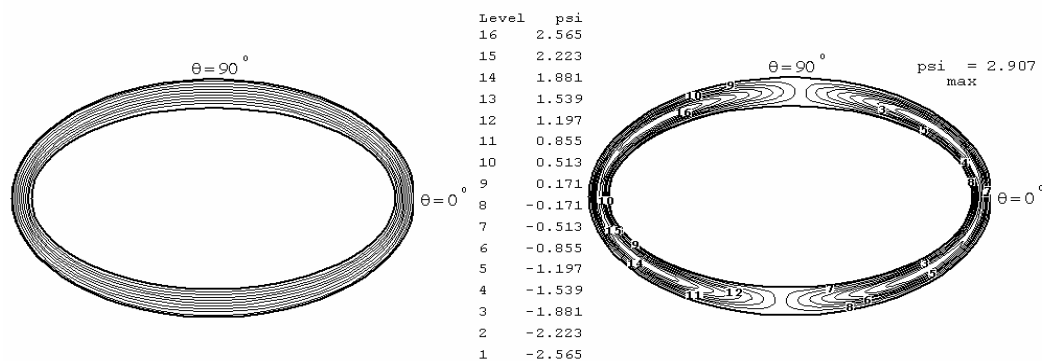Fig. 9: Isotherms and streamlines for $Gr = 2 \cdot 10^5$, $\alpha = 0°$, $e_1 = 0.9$ and $e_2 = 0.75$

Since this study examines the natural convection in an annulus whose geometry varies with eccentricity, the equivalent conductivity is the most suitable parameter with which to compare the surface heat transfers of the various annular spaces. The equivalent conductivity is defined as :

$$\lambda^*_{eq} = \frac{\left.\dfrac{\partial T^*}{\partial \eta}\right|_{convection}}{\left.\dfrac{\partial T^*}{\partial \eta}\right|_{conduction}}$$

The Nusselt number is proportional to the overall value of heat transfer rate which consists of both conductive and convective modes; whereas the equivalent conductivity represents the ratio of total heat transfer between the inner and outer cylinders, the Nusselt number is not a good indicator of heat transfer when comparing different geometries.

The local equivalent conductivity is defined as the ratio of the local Nusselt number on the surface over which a fluid is moving to the local Nusselt number which would be calculated if the fluid were quiescent. The overall equivalent conductivity is given by the ratio of the average Nusselt numbers for either case.

Table 2 gathers the overall equivalent conductivities for all the cases examined, on the internal wall.

Table 2: $\overline{\lambda^*_{eq}}$ for all the cases examined in this paper

e_1	$\downarrow \alpha$ $Gr \rightarrow$	10^3	10^4	10^5	10^6
0.999	0 °	1.001	1.183	1.849	**2.448**
0.9	0 °	1.000	1.000	1.221	1.444
0.83	0 °	1.000	1.000	1.000	1.001

Figure 10 shows that the average equivalent conductivity values on the internal wall increase with the increasing of the internal eccentricity.
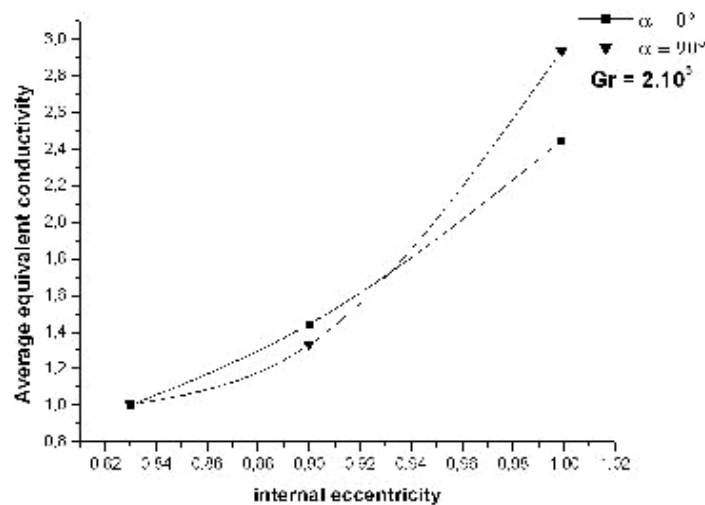

Fig. 10: Average equivalent conductivity on the internal wall

5. CONCLUSION

The suggested calculation code, which uses the method of finite volumes, with the velocity-pressure formulation, makes it possible to find with a good agreement, the literature results, which solve problems similar to that studied. Thus we theoretically studied, the bidimensional thermal natural convection, in laminar flow and permanent, in an annular space located between two confocal elliptic cylinders. We examined, in particular, the influence, of the internal eccentricity on the convective mode. We considered one value of α: $\alpha = 0°$. Simulations were executed from four values of the Grashof number : $Gr = 10^3$, $Gr = 10^4$, $Gr = 10^5$ and $Gr = 2 \cdot 10^5$.

The results underline the influence of the internal eccentricity on the average equivalent conductivity ($\overline{\lambda^*_{eq}}$). The maximum value is obtained for $\alpha = 0°$ when $e_1 = 0.999$.

For low Grashof number values, the coefficient of heat transfer is dominated by the mechanism of the conduction for the considered values of e_1.

Acknowledgments:

NOMENCLATURE

A	:	Constant defined in the system of elliptic coordinates
		= characteristic length (m)
A_1, A_2	:	Length of major axis in internal and external cylinder (m)
B_1, B_2	:	Length of minor axis in internal and external cylinder (m)
c_p	:	Specific heat at constant pressure ($J.kg^{-1}.K^{-1}$)
e_1, e_2	:	Eccentricities of ellipses
Nu, $\overline{Nu}$	:	Local and average Nusselt number
P	:	Pressure (Pa)
Ra	:	Rayleigh number, $Ra = Gr\,Pr$
T	:	Fluid's temperature (K)
T_1, T_2	:	Temperature of the wall of elliptic internal and external cylinder (K)
ΔT	:	Temperature difference between the inner and the outer wall,
		$\Delta T = T_1 - T_2$ (K)
t	:	Time (s)
u, v	:	Velocities components according to coordinates x and y ($m.s^{-1}$)
V_η, V_θ	:	Velocities components according to coordinates η and θ ($m.s^{-1}$)
$\vec{V}$	:	Velocity vector ($m.s^{-1}$)
x, y, z	:	Cartesian coordinates (m)

Greek letters

α	:	Angle of inclination between OH and OX (fig. 1) (°)
β	:	Thermal expansion coefficient (K^{-1})
λ	:	Thermal conductivity ($W.m^{-1}.K^{-1}$)
$\overline{\lambda^*_{eq}}$	:	Average equivalent thermal conductivity
ν	:	Kinematic viscosity ($m^2.s^{-1}$)
ρ	:	Density ($kg.m^{-3}$)

π   : Stress tensor
η, θ, z   : Elliptic coordinates
ψ   : Stream function ($m^2.s^{-1}$)
Exponents
*   : Dimensionless parameters
Indices
i and 1   : Interior
e and 2   : Exterior

REFERENCES

[1] L.R. Mack and E.H. Bishop, "*Natural Convection Between Horizontal Concentric Cylinders for Low Rayleigh Numbers*", Quart. Journ. Mech. And applied Math., XXI, pp. 223-241, 1968.

[2] T.H. Kuehn and R.J. Goldstein, "*An Experimental and Theoretical Study of Natural Convection in the Annulus Between Horizontal Concentric Cylinders*", J. Fluid. Mech., 74, pp. 695-719, 1976.

[3] J.H. Lee and T.S. Lee, "*Natural Convection in the Annuli Between Horizontal Confocal Elliptical Cylinder*", Int. J. Heat. Mass. Trans., 24, pp. 1739-1742, 1981.

[4] M.M; Elshamy, M.N. Ozisik and J.P. Coulter, "*Correlation for Laminar Natural Convection Between Confocal Horizontal Elliptical Cylinders*", Num. Heat. Trans. A 18, pp. 95-112, 1990.

[5] W. Chmaissem, S.J. Suh and M. Daguenet, "*Numerical Study of the Boussinesq Model of Natural Convection in an Annular Space: Having an Horizontal Axis Bounded by Circular and Elliptical Isothermal Cylinders*", App. Therm. Engin., 22, pp. 1013-1025, 2002.

[6] C.H. Cheng and C.C. Chao, "*Numerical Prediction of the Buoyancy-Driven Flow in the Annulus Between Horizontal Eccentric Elliptical Cylinders*", Num. Heat. Trans. A 30, pp.283-303, 1996.

[7] G. Guj and F. Stella, "*Vorticity-Velocity Formulation in the Computation of Flows in Multiconnected Domains*", Int. J. Numer. Meth. Fluids., 9, pp.1285-1298, 1989.

[8] Y.D. Zhu, C. Shu, J. Qiu and J. Tani, "*Numerical Simulation of Natural Convection Between Two Elliptical Cylinders Using DQ Method*", Int. J. Heat. Mass. Trans., 47, pp. 797-808, 2004.

[9] S.V. Patankar, "*Numerical Heat Transfer and Fluid Flow*", McGraw-Hill Book Company, New York, 1980.